CHAPTER II
LITERATURE REVIEW

2.1 Smart Packaging

Intelligent packaging is in an early stage of development technology that uses the communication function of the package to facilitate decision making to achieve the benefits of enhanced food safety and quality. In recent years, Intelligent Packaging and Smart Packaging terms have begun to appear. The definition of these terms is often used interchangeably but generally they are used with different meanings. Intelligent packaging could be defined as a packaging system that sensed and communicated, while smart packaging as one that possessed the capabilities of both intelligent and active packaging. Another definition for intelligent packaging is a packaging that monitors the conditions of packaged foods to give information about the quality of the food during storage and transport.

Intelligent packaging could also be defined; as a packaging system that is capable of carrying out intelligent functions (such as sensing, detecting, tracing, recording and communicating) to facilitate decision making to extend shelf life, improve quality, enhance safety, provide information, and warn about possible problems. A package can be intelligent if it has the ability to track the product, sense the environment inside or outside the package, and communicate with human. For example, an intelligent package can monitor the safety and quality condition of a food product and provide early warning to the consumer or food manufacturer. Intelligent packaging could be defined as a packaging technique containing an external or internal indicator for the active product quality and history.

Intelligent packaging system can be divided into three main groups as follows. (Otles *et al.*, 2008).

2.1.1 Gas Sensors

Gas sensors are devices which respond reversibly and quantitatively to gaseous analytes by changing the physical parameters of the sensor. Systems currently available for gas detection include amperometric oxygen sensors, potentiometric carbon dioxide sensors, metal oxide semiconductor field effect

transistors, organic conducting polymers and piezo-electric crystal sensors. Conventional systems for oxygen sensors based on electrochemical methods have a number of limitations including consumption of analyte (oxygen), cross-sensitivity to carbon dioxide and hydrogen sulphide and fouling of sensor membranes. They also involve destructive analysis of packages.

In recent years, a number of instruments and materials for optical oxygen sensing have been reported. Such sensors are usually comprised of a solid-state material and operate on the principle of luminescence quenching or absorbance changes caused by direct contact with the analyte. They are chemically inert, do not consume analytes, and provide a non-invasive technique for gas analysis through translucent materials.

Approaches to opto-chemical sensing include (Kerry *et al.*, 2008): a fluorescence-based system using a pH sensitive indicator, absorption-based colorimetric sensing realized through a visual indicator, and an energy transfer approach using phase fluorimetric detection. The latter allows for the possibility of combining oxygen and carbon dioxide measurements in a single sensor through compatibility with previously developed oxygen sensing technology. Most carbon dioxide sensors, however, have been developed for biomedical applications and the use of existing carbon dioxide sensors in food packaging applications is currently not feasible.

2.1.2 Indicators

Indicators may be defined as substances which indicate the presence, absence or concentration of another substance, or the degree of reaction between two or more substances by means of a characteristic change, especially in colour. By contrast with sensors, indicators are not composed of receptor and transducer components and communicate information directly through a visual change. A number of commercially available indicators are available for use with packaged meats and meat products.

Freshness indicators provide direct product quality information resulting from microbial growth or chemical changes within a food product. Microbiological quality may be determined through reactions between indicators placed within the package and microbial growth metabolites. The number of

practical concepts of intelligent package indicators for freshness detection is limited; however, potential exists for the development of freshness indicators based on established knowledge of quality indicating metabolites. The improved detection of biochemical changes during storage and spoilage of foods provide the basis by which freshness indicators may be developed based on target metabolites associated with microbiologically-induced deterioration. The formation of different potential indicator metabolites in meat products is dependent on the interaction between product type, associated spoilage flora, storage conditions and the packaging system.

Freshness indicators based on broad spectrum colour changes have a number of disadvantages which need to be resolved before widespread commercial uptake is likely. A lack of specificity means that colour changes indicating contamination can occur in products free from any significant sensory or quality deterioration. The presence of certain target metabolites is not necessarily an indication of poor quality. More exact correlations need to be established between target metabolite, product type and organo-leptic quality and safety. The possibilities of false-negatives are likely to dissuade producers from adopting indicators unless specific indication of actual spoilage can be guaranteed. (Kerry *et al.*, 2008)

2.2 Polypropylene for Packaging

The structure of PP is a carbon chain with every other side group being a methyl (CH_3) instead of a hydrogen as with PE. This structure results in a harder and more resilient polymer than HDPE with permeability to water vapor and gases between those of LDPE and HDPE. The structure of PP can be varied several ways, including oriented or non-oriented, and can be extruded and coated to become heat sealable and change other film properties. The main application for meat packaging is in cook-in products, due to PP is high heat tolerance and impermeability to moisture during water bath or steam cooking. (Dawson, 2001).

Polypropylene is one of the fastest growing classes of thermoplastics. This growth is attributed to its attractive combination of low cost, low density, and high heat distortion temperature (HDT). The extraordinary versatility of unfilled virgin resin and reinforced polypropylene suits a wide spectrum of end-use applications for

fibers, films, and molded parts. However, there always exist certain shortcomings in physical and chemical properties that can limit universal use of any given polymer resin. In packaging, for example, polypropylene resins have poor oxygen barriers, while low dimensional and thermal stability limits the scope of polypropylene composites in automotive applications. Most schemes to improve polypropylene gas barrier properties involve either addition of higher barrier plastics via a multilayer structure or surface coatings. Although effective, the increased cost of these approaches negates one big attraction for using polypropylene in the first place economy (Mirabella, 2009).

Table 2.1 Plastics used for packaging meat product

Polymer type	Use	Features
Ionomer	Heat-seal layer	Resists seal contamination
Nylon (uncoated)	Films, thermoformed trays	Also used as bone guards
Nylon (PVdC[1] coated)	Films, thermoformed trays	
PETE[1] (uncoated)	Films, trays	Good clarity
PETE[1] (PVdC coated)	Films	
LDPE[1]	Bags, wraps	Low cost, low gas barrier
LLDPE[1]	Heat-seal layer	Good clarity
EVA[1]-LDPE copolymer	Seal layer, films, wraps	Heat shrinkable
PP[1] (non-oriented)	Semi-rigid containers	
PVC[1]	Fresh meat wrap	Gas transmission rate depends on plasticization
PVdC	Barrier layer	Barrier less affected by moisture

[1]PVdC, polyvinyldienechloride; PETE, polyethylene terephthalate (polyester); LDPE, low density polyethylene; EVA, ethylene vinyl acetate; LLDPE, linear low density polyethylene; PP, polypropylene; PVC, polyvinyl chloride.

2.3 Clay Minerals

During the last decade, interest in polymer-layered silicate (PLS) nanocomposites has rapidly been increasing at an unprecedented level, both in industry and in academia, due to their potential for enhanced physical, chemical, and mechanical properties compared to conventionally filled composites. They have the

potential of being a low-cost alternative to high-performance composites for commercial applications in both the automotive and packaging industries. Polymer nanocomposites are two-phase materials in which the polymers are reinforced by nanoscalellers. The most heavily used filler material is based on the smectite class of aluminum silicate clays, of which the most common representative is montmorillonite (MMT). MMT has been employed in many PLS nanocomposite systems because it has a potentially high-aspect ratio and high-surface area that could lead to materials which could possibly exhibit great property enhancements. In addition, it is environmentally friendly, naturally occurring, and readily available in large quantities. Layered silicates in their pristine state are hydrophilic. Most of the engineering polymers are hydrophobic. Therefore, dispersion of native clays in most polymers is not easily achieved due to the intrinsic incompatibility of hydrophilic-layered silicates and hydrophobic engineering polymers.(Nguyen *et al.*, 2006).

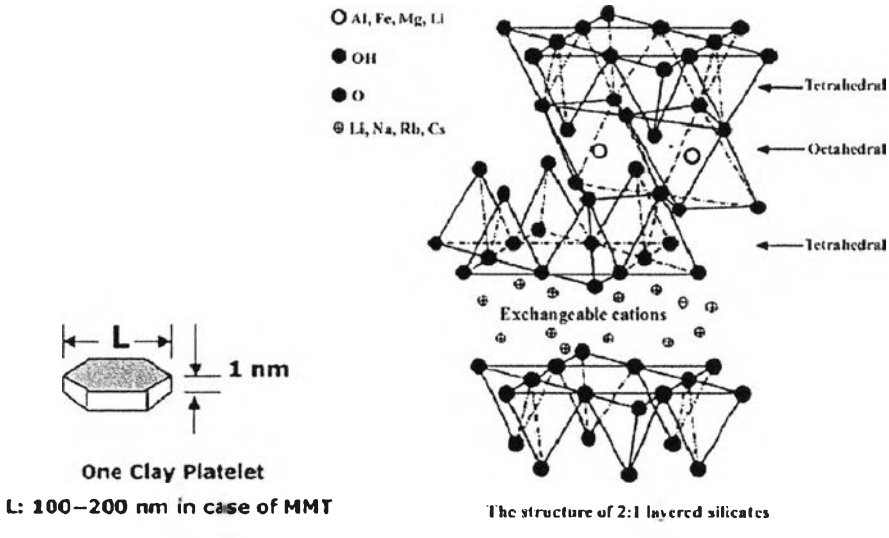

Figure 2.1 Structure of montmorillonite (Nguyen *et al.*, 2006).

Smectic clay is phyllosilicates or layer silicates having a layer lattice structure in which two-dimensional oxoanions are separated by hydrated cations. Montmorillonite, which is the main constituent of bentonites, is a mainly species of smectite clay. The structure is made of several stacked layers, with a layer thickness around 0.96 nm and lateral dimension of 100-200 nm. These layers organize

themselves to form the stacks with a regular gap between them, called interlayer or gallery. The sum of the single layer thickness (0.96 nm) and the interlayer represents the repeat unit of the multilayer material, called d-spacing or basal spacing (d_{001}) and is calculated from the (001) harmonics obtained from X-ray diffraction patterns (Lertwimolnum *et al.*, 2005). Its crystal lattice consists of a central octahedral sheet of alumina fused between two external silica tetrahedral sheets, as shown in Fig.2.1

Bentonite is impure clay consisting mostly of montmorillonite. There are different types of bentonite, each named after the respective dominant element, such as potassium (K), sodium (Na), calcium (Ca), and aluminium (Al). Bentonite usually forms from weathering of volcanic ash, most often in the presence of water. For industrial purposes, two main classes of bentonite exist: sodium and calcium bentonite. Other common clay species, and sometimes dominant, are montmorillonite and kaolinite. Kaolinite-dominated clays are commonly referred to as tonsteins and are typically associated with coal. Sodium bentonite expands when wet, absorbing as much as several times its dry mass in water. Sodium bentonite can also be "sandwiched" between synthetic materials to create geo-synthetic clay liners (GCL) for the aforementioned purposes. This technique allows for more convenient transport and installation, and it greatly reduces the volume of sodium bentonite required. Various surface modifications to sodium bentonite improve some rheological or sealing performance in geoenviromental applications, for example, the addition of polymers.

In order to have a successful development of clay-based nanocomposites, it is necessary to chemically modify a naturally hydrophilic silicate surface to an organo philic one so that it can be compatible with a chosen polymer matrix. Generally, this can be done through ion-exchange reactions by replacing interlayer cations with quarternary alkylammonium or alkylphosphoniumcations (Fig.2.2). Ion-exchange reactions with cationic surfactants such as those mentioned above render the normally hydrophilic silicate surface organophilic, thus making it more compatible with nonpolar polymers. These cationic surfactants modify interlayer interactions by lowering the surface energy of the inorganic component and improve the wetting characteristics with the polymer.

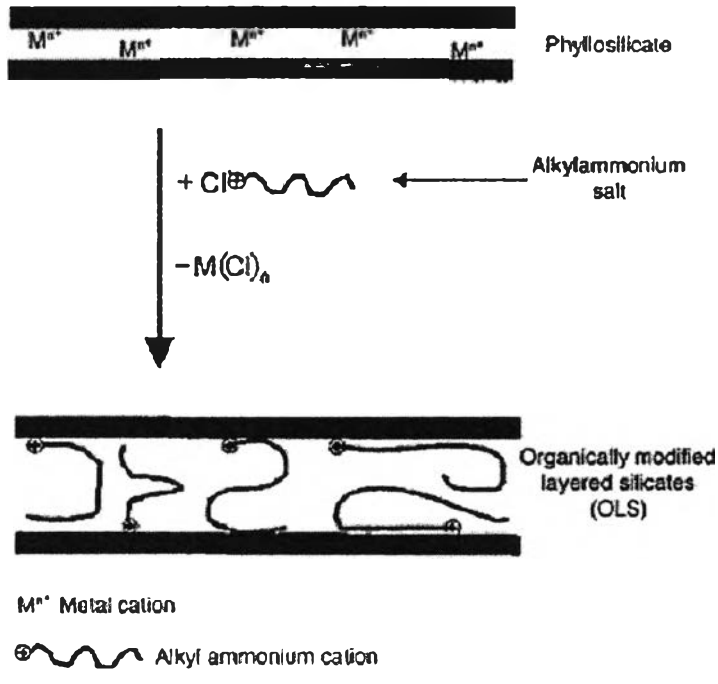

Figure 2.2 Representation of a cation-exchange reaction between the silicate and an alkylammonium salt (Nguyen *et al.*, 2006).

2.4 Polymer-Clay Nanocomposites Preparation

There are several processes to make polymer/clay nanocomposites, including in-situ polymerization, solution exfoliation and melt intercalation. As shown in Fig.2.3, each technique consists of several steps to achieve polymer nanocomposites and begin with organoclays or sometimes pristine clays.

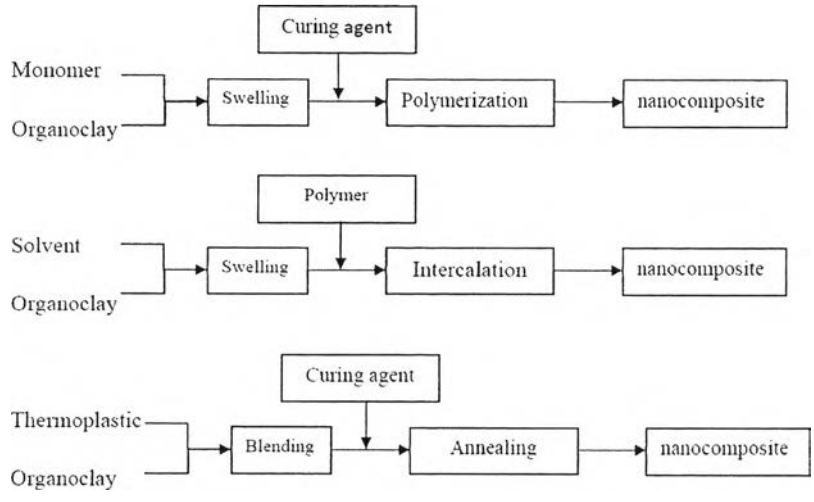

Figure 2.3 Flowchart of three processing techniques for clay-based polymer nanocomposite: in-situ polymerization (upper), Solution exfoliation (middle) and melt intercalation (bottom).

Nanocomposite structures depending on the nature of the components used (layered silicate, organic cation and polymer matrix) and the method of preparation, three main types of composites may be obtained when a layered clay is associated with a polymer (Fig.2.3). When the polymer is unable to intercalate between the silicate sheets, a phase separated composite (Fig.2.4a) is obtained, whose properties stay in the same range as traditional microcomposites. Beyond this classical family of composites, two types of nanocomposites can be recovered. Intercalated structure (Fig.2.4b) in which a single (and sometimes more than one) extended polymer chain is intercalated between the silicate layers resulting in a well ordered multilayer morphology built up with alternating polymeric and inorganic layers. When the silicate layers are completely and uniformly dispersed in a continuous polymer matrix, an exfoliated or delaminated structure is obtained (Fig.2.4c).

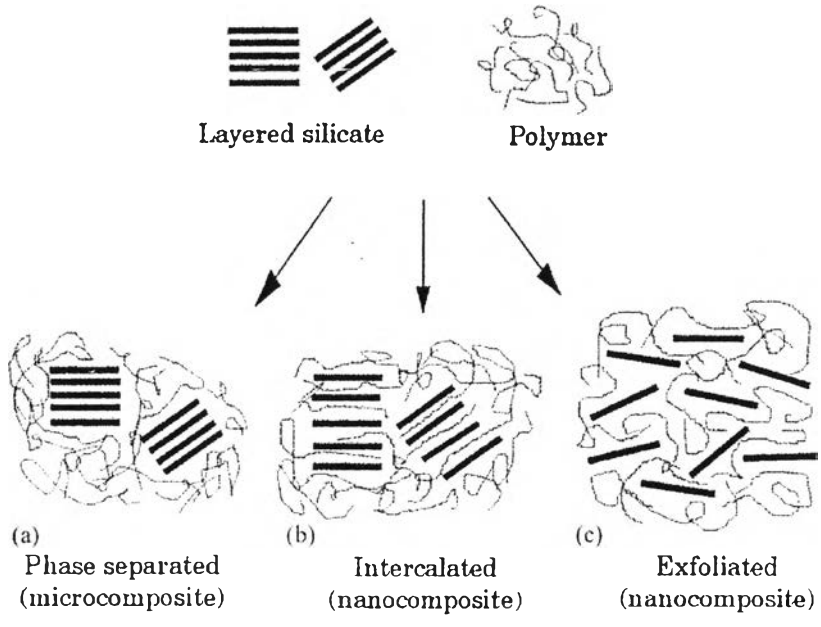

Figure 2.4 Scheme of different types of composite arising from the interaction of layered silicates and polymer : a) phase-separated mocrocomposite; b) intercalated nanocomposite and c) exfoliated nanocomposite (Alexandre *et al.*, 2000).

However, in this case of PP, it is frequently necessary to use a compatibilizer. The use of a compatibilizer, namely a chemical able to render compatible two different materials, made it possible for the melt intercalation technique to be accepted as the most promising approach leading to polymer-clay nanocomposites formation. In this way the use of solvent and dedicated processes could be avoided providing a formation procedure which is both environmentally and user friendly. It is important, at this point, to clarify that the surface treatment and the compatibilizer are two different, independent and complementary ways adopted to solve the problem of poor miscibility between PP and clay. Through the surface treatment it is possible to change the interlayer structure of clay both increasing the gallery gap and modifying the silicate surface in an organic fashion, but this artifice is not enough to render compatible matrix and filler: the polarizing compatibilizer needs to be introduced in the PP (Alexandre *et al.*, 2000).

Lertwimolnum *et al.* (2005) studied the effect of PP-g-MA concentration in the system polypropylene/organoclay and characterized the influence of processing conditions on clay dispersion. Polypropylene/organoclay nanocomposites have been prepared via direct melt intercalation in an internal mixer and a co-rotating twin screw extruder. Maleic anhydride grafted polypropylene (PP-g-MA) was used as a compatibilizer to improve the dispersability of the clay. The degree of dispersion is improved by incorporating a maleic anhydride grafted polypropylene (PP-g-MA). However, this improvement is obtained for concentrations of PP-g-MA higher than 10 wt%. The clay aggregates become smaller and silicate layers are finely dispersed, as the ratio of PP-g-MA increases. However, no further improvement on the dispersibility is observed for PP-g-MA content above 25 wt%. The effects of processing parameters are also investigated. The state of intercalation, interpreted by interlayer spacing, is globally unaffected by processing parameters. Increasing shear stress, mixing time and decreasing mixing temperature improve clay layer silicate exfoliation. The proportion of exfoliation is characterized by rheological measurements. A Carreaun Yasuda model with yield stress is used to describe the behavior at low frequency. It is shown that the yield stress value is directly correlated to the degree of exfoliation of nanocomposites.

Garcia-Lopez D *et al.* (2003) studied effect of compatibilizing agent on clay dispersing based on PP/clay nanocomposites. In this work, two different polar coupling agents, diethyl maleate grafted PP (PPgDEM) and commercial maleic anhydride grafted PP (PPgMA) have been used. The choice of diethyl maleate (DEM) as compatibilizing agent has been made because of its high thermal stability, high boiling point and good compatibilization with polyolefins, compared with other compatibilizing agents. Furthermore, the low homopolymerization behavior of DEM, allows a better control of the functionalization reaction. Maleic anhydride (MAH) has been widely used as compatibilizing agent for this kind of systems and it is used as reference on this work. The PP-clay nanocomposites have been prepared by melt compounding with two different clays, commercial modified montmorillonite, and sodium bentonite (BNa) modified with octadecylammonium ions. Although the commercial clay outperforms octadecylammonium treated bentonite, differences in mechanical properties when using different clays were smaller if DEM was used

instead of MAH. This was a consequence of the very low degree of compatibilization between the polymer matrix and the clay. Clay dispersion and interfacial adhesion are greatly affected by the kind of matrix modification. Clay-matrix-oligomer system with DEM has lower polarity compared with MAH, providing a less effective interaction with the polar components of the clay. The reactivity of MAH towards the modifying agent is greater than in the case of DEM. Both factors give as result better interfacial adhesion and subsequent mechanical performance for MAH nanocomposites.(Mirabella, 2009).

Halimatudahliana *et al.* (2003) studied four types of compatibilizers (polystyrene-block–poly(ethylene–butylene)-block–polystyrene (SEBS), Surlyn®, ethylene vinyl acetate (EVA), sodium salt hydrate of 4 styrenesulfonic acid (4ssa,ssh) with concentration of 7.5%w/w) to improvements in properties through an affinity and polarity concept. The effect of various compatibilizers on the mechanical properties of polystyrene/polypropylene (PS/PP) blends was investigated. Blends of 20/80, 50/50 and 80/20 (wt%) were prepared through melt blending in a single screw extruder at a blend temperature of 200°C and a screw speed of 40 rpm. It could be concluded that those blends with 7.5% SEBS produce an improvement in toughness of PS/PP blends for all blend compositions. Moreover, the brittle behavior can be converted into a quite ductile material in 50/50 and 80/20 PS/PP blend with the addition of SEBS. The addition of 7.5% Surlyn® increased the tensile strength and Young's modulus of the blend. In the case of adding 7.5% of EVA in PS/PP blend, the results indicated that a slight improvement in elongation at break was obtained, whereas in corporation of 7.5% of EVA has reduced the properties in all blend compositions.

Tassanawat *et al. (2006)* studied the processing of pH-sensitive material used for milk packaging based on polypropylene/organoclay nanocomposites incorporated with indicator dyes. The nanoclay composites with indicator dyes were compounding through a twin screw extruder using Surlyn® as a compatibilizer. The nanoclay composites were fabricated into the sample sheet for the color testing and characterizations including thermal and mechanical properties. Milk deterioration was assessed for titratable acidity (TA), and color change of the film were measured

and expressed as Hunter values as well as total color different (TCD). TCD value of BMB (Bromothymol blue) and BP (Bromocresol purple) type-films also changed continuously with the response of the film. The color change of the films correlated well with TA value of fresh milk. According to the changes in Hunter color value of the films within the packages of fresh milk during storage at ambient temperature, the result showed that the color of BMB type-film turned from green to yellow whereas those of BP type-film turned from violet to green. The color changes of the developed indicator properly represented the degree of deterioration of fresh milk. Consequently, the nanocomposite indicator film could be employed as an effective smart packaging technology for evaluating fresh milk.

2.5 Synthesis of Copper Nanoparticle

Metallic Cu nanoparticles are attractive materials fundamentally and industrially because they give unique properties over catalysis, electronics, and photoelectronics, and their cost is low compared with other metallic materials such as gold and silver. The practical use of Cu nanoparticles faces at the main difficulty that arises from their instability toward oxidation in air. In addition, colloidal instability of nanoparticles brings about aggregation of the nanoparticles, which spoils the unique properties of nanoparticles. Various methods for stabilizing the Cu nanoparticles have been reported. Several researchers have proposed the use of non-aqueous liquid such as organic compounds as solvent or dispersing media, which does not dissolve oxygen gas and prevents it from contacting Cu nanoparticles, so that the Cu surface oxidation would be minimized. Though their methods could avoid oxidation of Cu nanoparticles, harm and hazard of organic compounds are matter of concern.

Protection of Cu nanoparticles with a stabilizer such as surfactant can be given as another stabilization method, and various methods using the stabilizer have been previously reported. The nanoparticles are surrounded with the stabilizer by hydrophilic interaction between the nanoparticles and the stabilizer and/or coordination of functional groups of the stabilizer to metal atoms. However, the

stabilizer may not prevent oxidation and aggregation of nanoparticles enough because of their molecular motion.(Kobayashi *et al.*, 2009).

Wu *et al.* (Wu *et al.*, 2006) synthesized stable narrowly distributed copper nanoparticles in the presence of polyvinylpyrrolidone (PVP) as a stabilizer and without deoxygenated solution and without inert gas protection. The functions of ascorbic acid were acting as both reducing agent and antioxidant to reduce the metallic ion precursor and to effectively prevent the common oxidation process of the new born pure copper nanoclusters. TEM images exhibited copper nanoparticles consisting of nearly spherical with an average particle diameter of 3.4 nm and very narrow size distribution. The XRD spectrum of the as-synthesized copper nanoparticles in the experiment (Fig.2.5) had three main characteristic diffraction peaks for copper at 2θ=43.2, 50.4 and 74.0 degree. From UV/Vis response, the ratio of [PVP]/[Cu^{2+}] indicated that they played an important role in controlling the size, size distribution and morphology of the nanoparticles. They found that the suitable ratio was 0.01 M [Cu^{2+}] and 0.8 M [PVP]+0.4M[VC] and 0.8 M [PVP], [VC]/[Cu^{2+}] = 40, [PVP]/[Cu^{2+}] = 160. PVP was also verified as an ideal candidate for stabilizing and controlling the copper nanoclusters growth. Although the fundamental mechanism has yet to be fully described, it is believed that PVP can coordinate to the particles surface via O-Cu coordination bond and wrap around the particles with its long and soft polyvinyl chain to stop their growth and aggregation toward bulk particles.

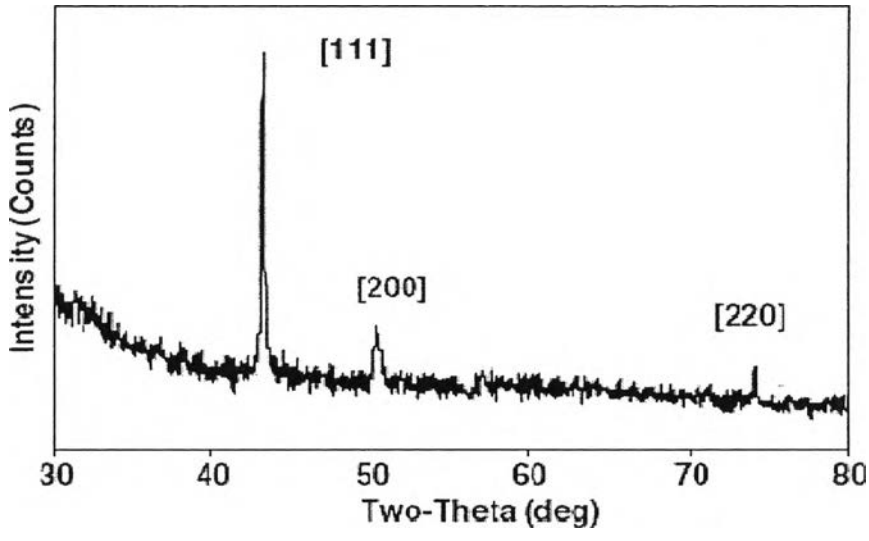

Figure 2.5 XRD pattern of copper nanoparticles (Wu *et al.*, 2006).

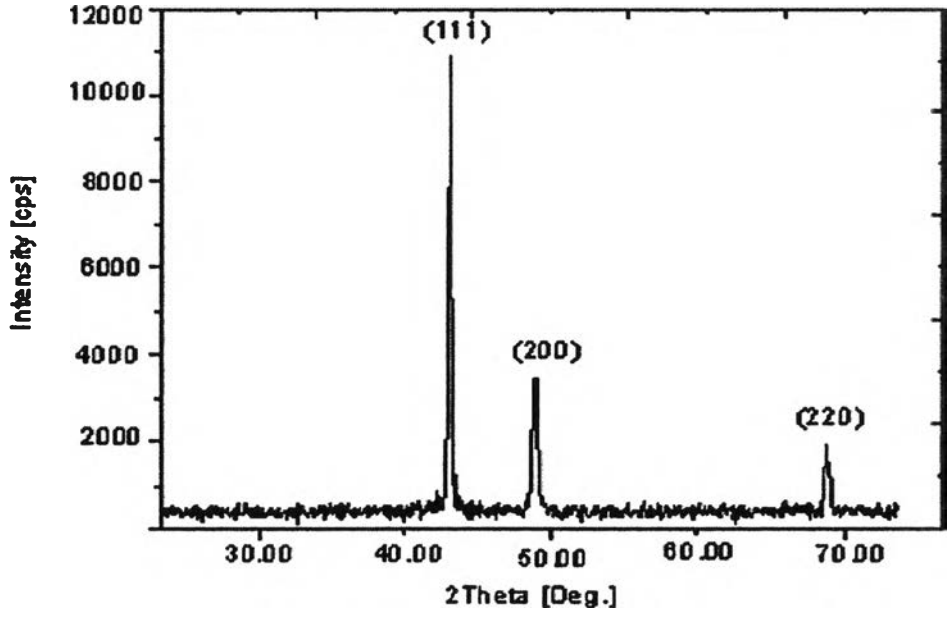

Figure 2.6 XRD pattern of copper nanoparticles (Wu, 2007).

Wu (2007) prepared ultrafine copper powder with chemical reduction method by using ascorbic acid as reducing agent and the pH value was controlled at 6 with aqueous ammonia for application in MLCC. The XRD pattern (Fig.2.6) of the

product prepared by the solution containing $CuSO_4 \cdot 5H_2O$ and ascorbic acid showing the characteristic peaks of crystalline metallic copper (fcc) d=2.0897, 1.8091, 1.2790, respectively, which is very close to that given by JCPDS file no. 4-836 (d=2.088, 1.808, 1.278). SEM images showed that the powder particles were polyhedral, non-agglomerated monodispersed, and their diameters were uniformly distributed below 2.7 μm for samples prepared at pH 2.2. When the pH value was up to 6, the particles were in the uniform size of 1.5 μm. Thus, the reducing power of ascorbic acid was pH-dependent and the particles size decreased with increasing pH value. The reductive power of ascorbic acid also depended on the reaction temperature greatly. The efficiency was stable and low to 20% in spite of the increase in pH value when the reaction temperature was lower than 50°C.When the reaction temperature was more than 50°C, the efficiency increased as the reaction temperature increased up to 92% at 70°C.

Giuffrida *et al.* (2008) studied the effect of the presence of poly(vinyl pyrrolidone) (PVP) on the copper nanoparticle formation, obtained by UV irradiation of ethanol solution of $Cu(acac)_2$ (acac = 2,4-pentanedionato). The size and the distribution of the copper particles were determined by DLS measurements. It was found that the mean size of the cluster decreased from 30 nm with a standard deviation = 12.5 nm to size of 9 nm with a standard deviation = 2.4 nm when the concentration increased from 0.02 M to 0.1 M, whereas the size distribution became very narrow. For higher PVP concentration, the mean size became smaller than 4 nm. Thus the PVP was an excellent controller of the copper particles obtained by sensitized photochemical reduction. The colloidal solution, stocked in inert atmosphere, was reported to be stable for months. The PVP is believed to act as a protective agent, probably the polymer wraps up the copper cluster via partial donation of oxygen lone pair of C=O groups to the vacant orbitals of the copper cluster surface.

Ruparelia *et al.* (2008) compared the bactericidal effect of silver and copper nanoparticles using various microbial strains. The copper nanoparticles were prepared by wet chemical synthesis involving stoichiometric reaction between sodium borohydride and copper ions. The nitrate salts of copper were used as precursors and reaction with sodium borohydride was conducted by vigorously

stirring the reaction mixture. After synthesis, the nanoparticles were washed twice with DI (deionised) water to ensure removal of residual boron. The average sizes of the copper nanoparticles were 9 nm as determined through transmission electron microscopy. Energy-dispersive X-ray spectra of copper nanoparticles revealed that an oxide layer existed on the copper nanoparticles.

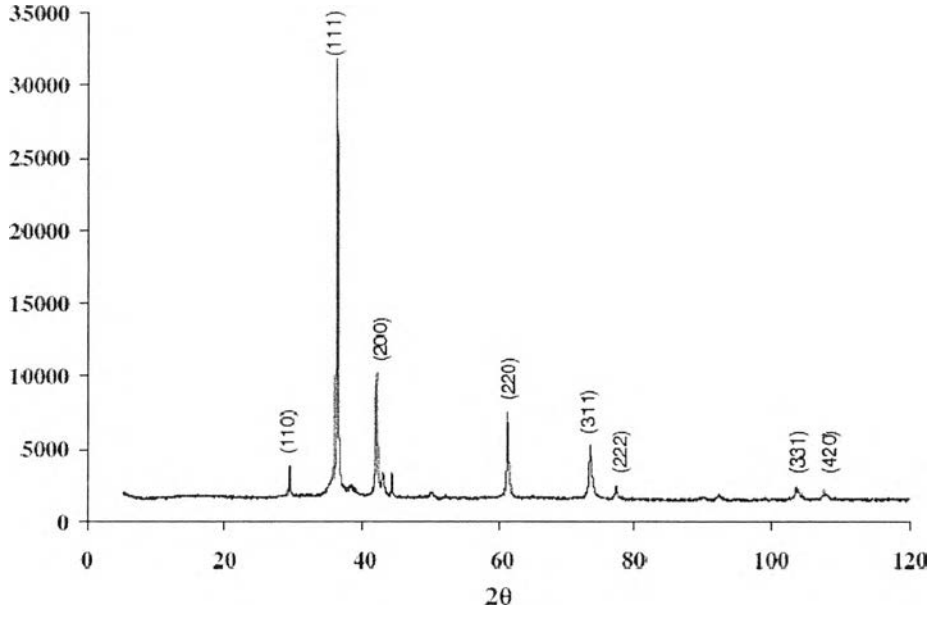

Figure 2.7 XRD pattern of copper oxide nanoparticles (cuprite or CuO).

The XRD pattern (Fig.2.7) of copper nanoparticles were compared and interpreted with standard data of International Centre of Diffraction Data (ICDD). The eight characteristic peaks for cuprite appeared in the sample of copper nanoparticles at 29.6, 36.3, 42.2, 61.3, 73.5, 77.5, 104.1, 108.8, which correspond to crystal facets of (110), (111), (200), (220), (311), (222), (331) and (420). Each crystallographic facet contains energetically distinct sites based on atom density. The copper nanoparticles contain high atom density facets such as (111) that are known to be highly reactive. The XRD patterns of copper nanoparticles confirm the presence of copper is present as cuprite.

Zhang *et al.* (2007) synthesized cuprous oxide (Cu_2O) nanostructures with different shapes, such as spheres, cubes and rods, by reducing copper nitrate

trihydrate with ethylene glycol in the present of poly(vinylypyrrolidone) (PVP). The molar ratio of PVP (in the repeating unit)/$Cu(NO_3)_2 \bullet 3H_2O$ and reaction temperature have significant effects on the formation and growth of these Cu_2O nanostructures. Fig.2.8 shows an XRD pattern of the as-prepared cuprous oxide cubes. All the peaks are labeled and can be readily indexed to a crystalline cubic phase Cu_2O with lattice constant a = 4.260 A^o (JCPDS 65-3288). The lattice constant was calculated by Scherrer formula to be a = 4.263A^o, which was consistent with the literature standard value.

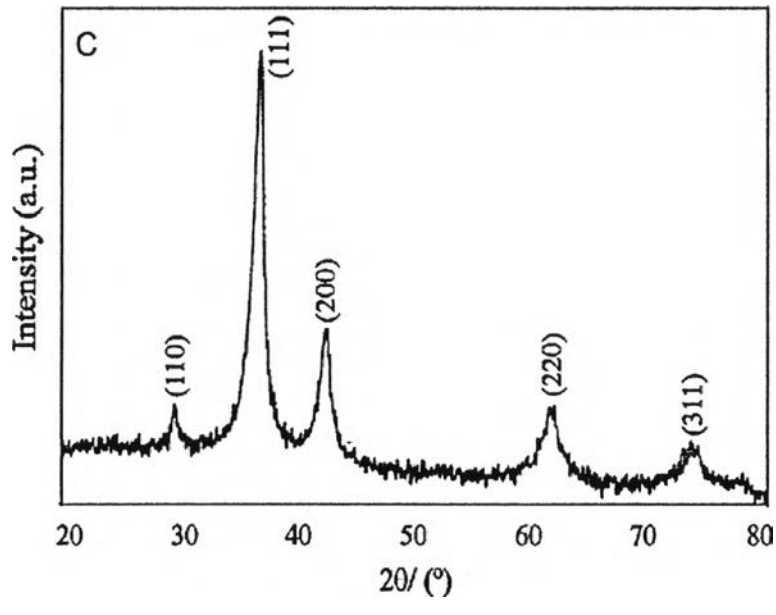

Figure 2.8 XRD pattern of the as-prepared cuprous oxide cubes. All the peaks are labeled and can be readily indexed to a crystalline cubic phase Cu_2O with lattice constant a= 4.260Å (JCPDS65-3288).

2.6 Fish Freshness

Fresh fish are one of the most perishable of all foods. The rate of spoilage rise with temperature. They must be refrigerated or frozen immediately after harvest and kept refrigerated until eaten. Spoilage of fish is not clearly defined. Obvious signs of spoilage are formation of off-odors and off-flavors, slime formation, gas

production and changes in texture. The development of these spoilage conditions in fish and fish products is due to a combination of microbiological, chemical and autolytic phenomena. Autolytic spoilage is responsible for the initial loss of quality in fresh fish, but contributes very little to spoilage of chilled fish and fish products. The decomposition of the fish occurs as its constituent compounds break down. The proteins, nucleotides and sugars break down, bases are released; the pH falls and the fats are oxidized. These make the fish smelly, rancid and tough. The physical, chemical, and bacteriological characteristics of fish vary with species, seasons, method of capture, fishing grounds etc. However, it is possible to describe the changes that take place after death, until the fish is totally spoiled and unfit for human consumption. The changes in fish have three main groups of causes: bacteria, digestive enzymes and others (e.g. oxidation leading to rancidity).

The retail food market in Thailand is changing rapidly; the number of shops handling a narrow range of foods is decreasing, while supermarkets and large self service stores are increasing in number and size. There is considerable scope for expanding the market for fish through these modern outlets, provided a good quality product is attractively presented for sale in a suitable package. Some large stores are selling wet fish from a traditional slab, with a fishmonger in attendance, but this method has a number of disadvantages; a large space is needed, the slab has to be manned continuously, the products are inconvenient to handle and there may be some smell and possibly contamination. In contrast, properly packaged fish products can be easily handled by nonspecialist staff, examined by the shopper for type, quantity and price, purchased and carried home in the shopping basket with other foods.

Prepacked chilled fish have been sold for many years from frozen food cabinets containing other foods. Prepacking is mainly a method of presentation, not of preservation; the shelf life of a wrapped wet fish product is virtually the same as that of an unwrapped one. There is sometimes a small increase in shelf life, but not enough to justify keeping prepacked fish longer in the shop. The most useful materials for making small packages of chilled fish are the thin flexible films produced mainly from plastics such as polyethylene, polypropylene, and polyvinyl chloride.

Chilled fresh fish requires the protection of a reasonably good barrier to water vapour to prevent it drying. Water vapour can pass through a film in two ways; the film may be porous so that vapour passes through holes in the material, or the film may be permeable, that is water vapour diffuses through it by dissolving in the material. Thin films are often porous, but porosity can be overcome by using a thicker film; however, a permeable film cannot be made impermeable in this way. Gases like oxygen or carbon dioxide for example are transmitted through a film in much the same way as water vapour.

2.7 Freshness Indicator

Pacquit *et al.* (2006) had developed "chemical bar-code" for real-time monitoring of fish freshness. A solid-state sensor contains a pH sensitive dye, bromocresol green, that responds through visible colour change (yellow to blue) to basic volatile spoilage compounds, such as trimethylamine (TMA), ammonia(NH) and dimethylamine (DMA) collectively known as Total Volatile Basic Nitrogen (TVB-N). The sensors were prepared by spin-coat sensor solution on optically clear PET discs under constant nitrogen flow at 1000, 2000 and 3000 rpm for approximately 10 min. Sensors were assembled by placing the coated spot face down in a sandwich between a poly tetrafluoroethylene (PTFE) gas permeable membrane and a clear protective adhesive cover above. Results indicated that the higher the spin-coating speed, the thinner the sensor with the average profilometer results being 2.57, 1.36 and 1.01 m at a spin rate of 1000, 2000 and 3000 rpm, respectively. The sensor characteristics were studied as well as its response with standard ammonia gas. The approach is sensitive to volatile amines, with a linear response to ammonia gas concentration from 0 to 15 ppm (Fig.2.9).

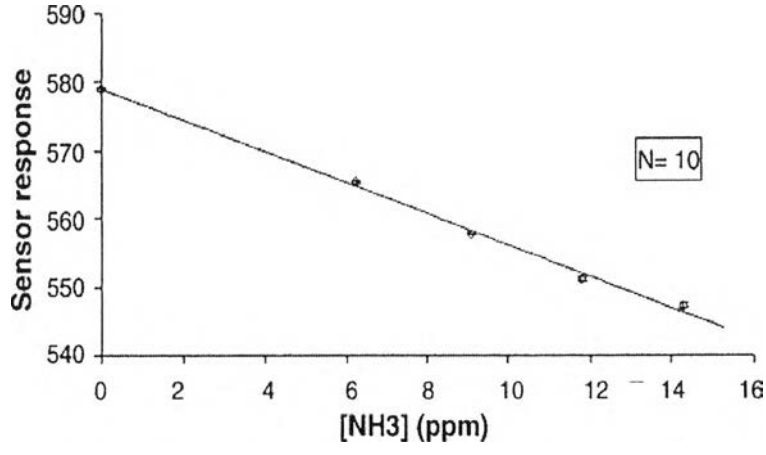

Figure 2.9 Sensor responses (spin-coated at 100 rpm) to ammonia concentration monitored by the optical scanner.

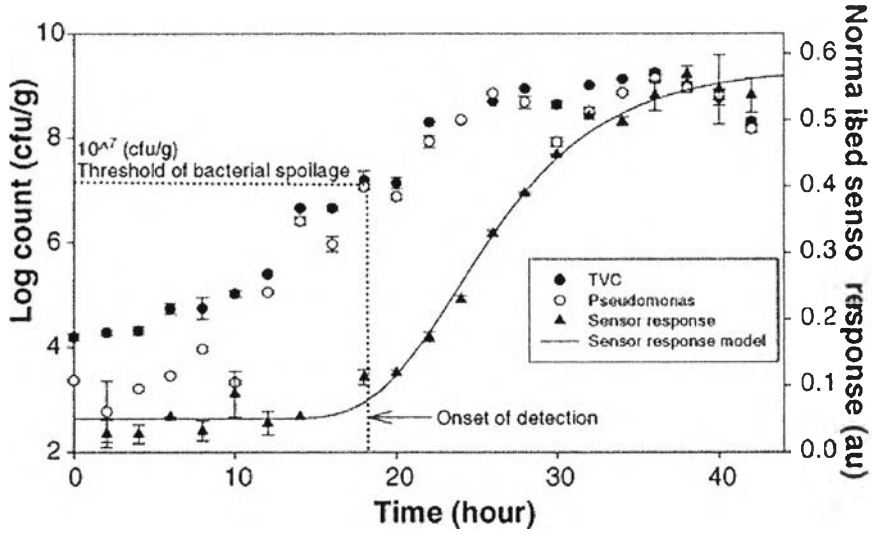

Figure 2.10 Correlation of sensor response (1000 rpm) and changes in bacterial population of fresh cod kept at 20 °C over time.

A delay between the rise in microbial population and the sensor response curves is also apparent from Fig.2.10. This delay is inherent as volatile base generation follows the increase in SSO population. Thus, the sensors accurately tracked the increase in volatile base concentration in the package head space and

since the region of change in sensor colour coincides with higher levels of SSO in the fish tissue, the scanner measurements of on-package sensor colour are useful indicators of approximate SSO population and therefore spoilage of the fish samples.

Pacquit *et al.* (2007) studied dye leaching of Bromocresal green and correlation between sensor response and microbial growth over time in fish caught at the beginning of the autumn. Two fish species (cod and whiting) were selected for investigation. Leaching studies show the effect of ammonium bromide salts on BCG leaching. Tetraoctyl ammonium bromide reduced leaching by 82% and was selected for the fish spoilage trial. Fig.2.11 shows the change in TVB-N level monitored by the color sensor in spoiling cod at room temperature. For the first 14 h, no color change was detected by the reflectance colorimeter but at 16-18 h, a denoted increase in reflectance was recorded. The sensor gradually changed color from yellow to green then to blue in approximately 43 h where no further color change was observed. Similar results were obtained with the whiting samples.

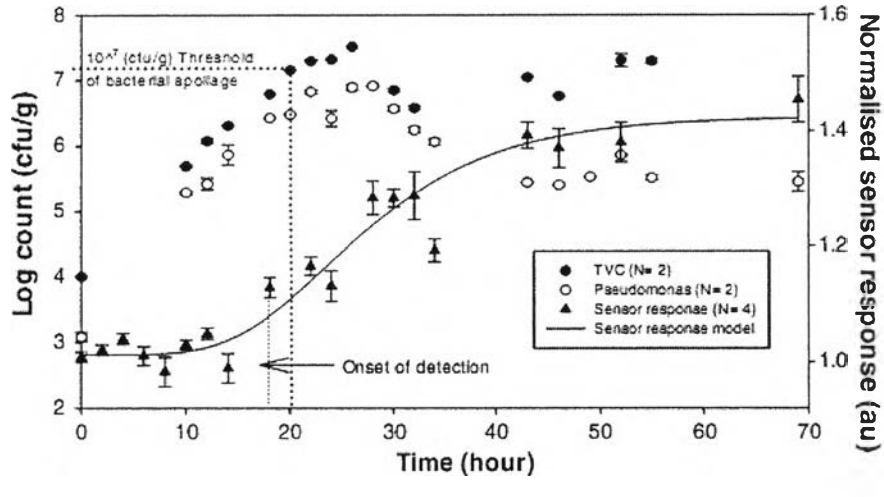

Figure 2.11 Normalized data showing the correlation between sensor response and bacterial population (TVC and Pseudomonas spp.) in cod filet samples at 21 ^{o}C. The error bars are SEM (standard error of the mean) values.

From microbial analysis shows ranges of microbial population commonly associated with spoilage in white fish and the specific level of 10^7 cfu/g was reached

after about 18 h in cod and 14 h in whiting. The TVC counts were found slowly increasing from approximately 10^4 cfu/g during the initial 10 h but sharply rising from then on, reaching values of 10^7 cfu/g at approximately 18 h before stabilizing at 26 h just above10^7 cfu/g. Clearly, this coincides with the onset of color change in the sensors (14-24 h) suggesting that the concentration of spoilage compounds in the headspace has reached the sensor lower detection limit. Thus, the sensors accurately track this increase in volatile base concentration in the package headspace.

Seok-In Hong *et al.* (2000)studied color indicators for kimchi packaging to evaluate the degree of fermentation of kimchi. Kimchi fermentation was assessed for titratable acidity (TA), and color changes of the indicators were measured and expressed as Hunter values as well as total color difference (TCD). TCD values of bromocresol purple (BP) type indicator (containing BP as a chemical dye) ranged 27-33. The developed color indicator film consisted of polypropylene (PP) resin, calcium hydroxide as a CO_2 absorbent, and bromocresol purple (BP) or methyl red (MR) as a chemical dye. The changes in TA of kimchi during fermentation at 0°C, 10°C, and 20°C were measured. The TA values of kimchi increased gradually at the initial stage and steeply at the middle stage, and remained constant at the final stage of fermentation, which had a sigmoid increase with increase in fermentation period. Changes in Hunter color values of the indicators within the packages of kimchi. In case of the indicator containing BP, Hunter *L* and *b* values increased gradually with storage time, while Hunter *a* value decreased slowly and then remained constant. However, Hunter *L* and *b* values of the indicator containing MR decreased exponentially, while Hunter *a* value increased remarkably and remained constant. The result means that color of the BP type indicator turned from initially blue to finally light green, and that of the MR type turned from light orange to red. The rate of the color changes was different depending on temperature. The result of correlation response of the indicator to kimchi fermentation suggests that the BP type indicator can be used successfully as a full time-fermentation indicator for kimchi products. However, the MR type may be applied only as a ripeness/unripeness indicator to packaged kimchi.

Two years later, Seok-In Hong *et al.* developed kimchi packaging by using gravure printed color indicators on common nylon/polyethylene (Ny/PE) film. A

gravure process was successfully applied as a novel approach to fabricate color indicators for kimchi packaging.

2.8 Natural Dye

A dye can be defined as a highly coloured substance used to impart colour to an infinite variety of materials like textiles, paper, wood, varnishes, leather, ink, fur, food-stuff, cosmetics, medicine, toothpaste, etc. As far as the chemistry of dyes is concerned, a dye molecule has two principal chemical groups, viz. chromophores and auxochromes. The chromophore, usually an aromatic ring, is associated with the colouring property. It has unsaturated bonds such as –C=C, =C=O, –C–S, =C–NH, –CH=N–, –N=N and –N=O, whose number decides the intensity of the colour. The auxochrome helps the dye molecule to combine with the substrate, thus imparting colour to the latter.

Natural dyes find use in the colouring of textiles, drugs, cosmetics, etc. Owing to their non-toxic effects, they are also used for colouring various food products. Natural dyes can be sorted into three categories: natural dyes obtained from plants, animals and minerals. Plants exhibit a wide range of colours, not all of these pigments can be used as dyes. Some do not dissolve in water, some cannot be adsorbed on-to fibres, whereas others fade when washed or exposed to air or sunlight.

Dyes are classified based on their chemical structure, sources, method of application, colour, etc. as a model study that explain the chemistry as described by Vankar. They are classified into the following groups based on chemical structure (Fig.2.12).

Indigo dyes: This is considered to be the most important dye obtained from the plant I. tinctoria L.

Anthroquinone dyes: Some of the most important red dyes are based on the anthroquinone structure. These are obtained from both plants and insects. These dyes have good fastness to light. They form complexes with metal salts and the resultant metal–complex dyes have good fastness.

Alpha-hydroxy naphthoquinones: The most prominent member of this class of dye is henna or lawsone (L. iner-mis L.).

Flavones: Most of the natural yellow colours are hydroxy and methoxy derivatives of flavones and isoflavones.

Dihydropyrans: Closely related to flavones in chemical structure are substituted dihydropyrans.

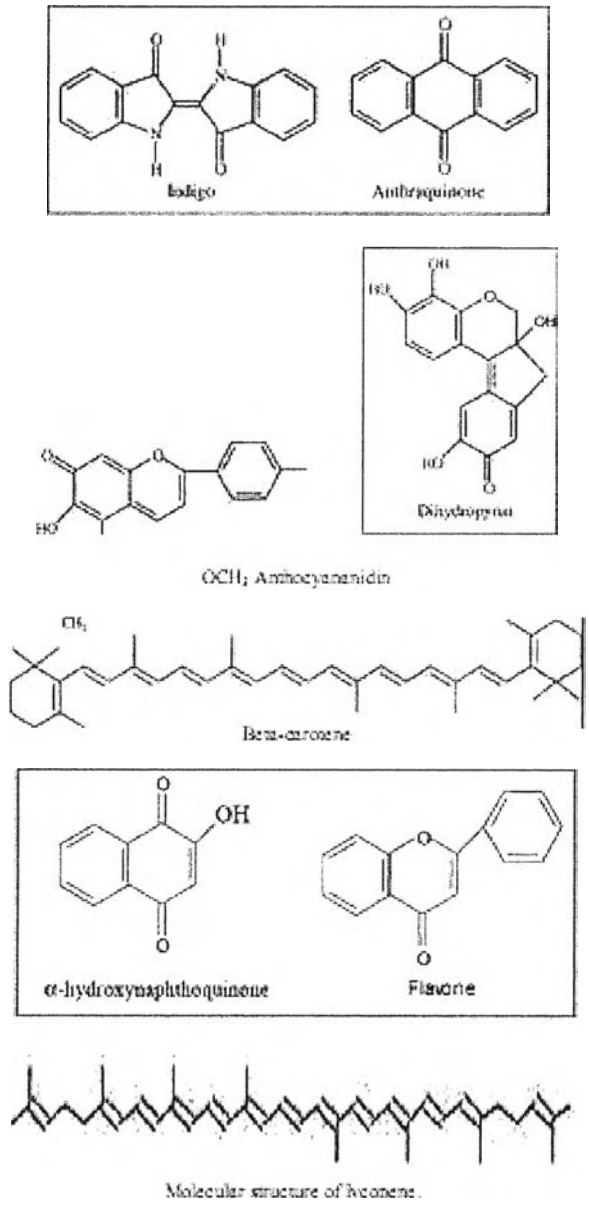

Figure 2.12 Example of molecular structure of natural dye.

Natural dyes are less toxic, less polluting, less health hazardous, non-carcinogenic and non-poisonous. Added to this they are harmonizing colours, gentle, soft and subtle, and create a restful effect. Above all, they are environment friendly and can be recycled after use. Although natural dyes have several advantages, there are some limitations as well. Some of the natural dyes are fugitive and need a mordant for enhancement of their fastness properties. Some of the metallic mordents are hazardous. Also there are problems like difficulty in the collection of plants, lack of standardization, lack of availability of precise technical knowledge of extracting and dyeing technique and species availability. (Siva, 2007).

2.9 Mangosteen and Dye from the Fruit Pericarp (hull) of Mangosteen

Mangosteen (*Garcinia mangostana* L.), a tropical evergreen tree growing in Malaysia, India, Thailand, Vietnam, Singapore, Philippines, and Burma, bears dark-purple to red-purple fruits. The edible portion of the fruit (aril) is white and soft with a slightly sour taste. The thickness of fruit pericarp (also referred as rind and skin) is 6-10 mm and it has been used in folk medicine for the relief of diarrhea, as well as for the treatment of skin wounds and disorders. Mangosteen fruit is a rich source of phenolic compounds, including xanthones, proanthocyanidins, anthocyanins, and phenolicacids. Of these, xanthones have been reported as the major phenolics found in the pericarp of mangosteen fruit. (M.Naczk *et al.*, 2011).

Mangosteen is famed as the Queen of tropical fruit because it is one of the best tasting fruits in the world. It can be cultivated in tropical areas especially in Thailand, Malaysia, the Philippines and Indonesia. Much research has revealed that extracts of Garcinia mangostana Linn have anti-inflammatory, antitumour, and antioxidant properties, as well as anti-bacterial activity. The fruit hulls of mangosteen are reported to be the source of α- and γ-mangostin, tannin, xanthone, chrysanthemin, garcinone, gartanin, vitamin B1, B2, C and other bioactive substances. Moreover, a substantial amount of red pigment was isolated from the fruit hulls of mangosteen. The major and minor pigments are cyanidin-3-sophoroside and cyanidin-3-glucoside respectively (Fig.2.13). The red pigment from the fruit hulls of mangosteen can be used as a natural dye source for dyeing, with associated

benefits in use with respect to reduced health hazards, lower toxicity and allergic reactions. (Chairat *et al.*, 2007).

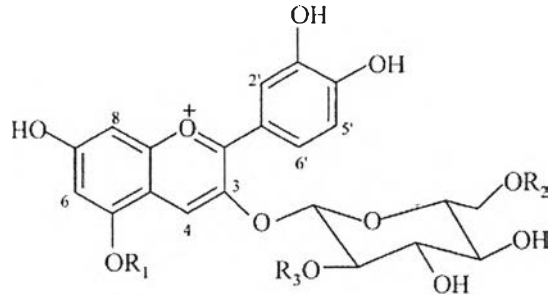

Figure 2.13 Chemical structure of cyaniding-3-glucoside (R_1=R_2=R_3=H) and cyaniding-3-sophoroside (R_1=R_2=H and R_3=glucosyl).

Siriwan (2004) studied the influence of the chitosan on dyeing properties of mangosteen rind on cotton fabric. The results of this study showed that the different solvents used for dye extraction provided different shades on dye fabrics. Water extractor gave brown shade while ethanol extractor gave yellow shade on dyed fabrics.

Sanida (2006) studied the antioxidant activity and quality from pericarps of mangosteen which included extraction, purification and test the oxidation activity of the extractive. The results showed that continuous extraction with Soxhlet apparatus significantly increased the yield (19.68% weight of ethanol extractive/ weight dry pericarp) of extractive as compared to merceration extractive (12.70% weight of ethanol eatractive/ weight dry pericarp). Further extract with ethyl acetate/ water yielded ethyl acetate extractives (14.53% weight of ethyl acetate extractive/weight dry pericarp). When separated the extractive with silica gel column chromatography yield 14 fractions. Pure compound from fraction B3 showed the best anti-oxidative effect. Characterization by IR, ^{1}H-NMR and ^{13}C-NMR techniques showed that the purified compound of B3 was α-mangosteen.

Chairat *et al.* (2007) studied dyeing of cotton and silk yarn by natural dye extracted from the dried fruit hulls of mangosteen. The optimal conditions for dye

extraction were to extract the dried fruit hulls of mangosteen at 80°C for 1 hour with a 15% w/v citric acid solution in a ratio of mangosteen powder to solvent of 1:4. The dye solution gave dark red color. It was kept cold at 5°C for further use. After filtration and dilution, the dye solution showed a maximum absorption peak (λ_{max}) at 510 nm in the visible spectrum.

M. Naczk *et al.* (2011) studied the affinity of crude extracts of phenolics (CP), isolated from mangosteen fruit parts. Furthermore, the antioxidant potential of mangosteen CP was also investigated. CP was extracted from peel, rind, and edible aril with 70% (v/v) aqueous acetone, three times, at room temperature for 30 min at a solid-to solvent ratio of 15:100 (w/v). The acetone extracts were cooled, evaporated to near dryness under vacuum at 40 °C, and then lyophilised. Following this, the dried CP were weighed to determine the extraction yields and stored at 18 °C until analyzed. The results showed that the rind and peel of mangosteen fruit contained over 20 times more phenolics than did the edible aril of the fruit.

2.10 References

Alexandre, M. and Dubois, P., (2000) Polymer-layered silicate nanocomposites: preparation, properties and uses of a new class of materials, Materials Scienec and Engineering, 28, 1-63.

Chairat, M. , Bremner, J.B. and Chantrapromma, K., (2007) Dyeing of cotton and silk yarn with the extracted dye from the fruit hulls of mangosteen, Garcinia mangostana Linn, Fibers and Polymers, 8 (6), 613-619.

Garcia-Lopez D., P.O., Merino J.C., Pastor J.M., (2003) Polyproplylene-clay nanocomposites: effect of compatibilizing agents on clay dispersion, European Polymer Journal, 39, 945-950.

Giuffrida, S., Costanzo, L., Ventimiglia, G., and Bongiorno, C. (2008) Photochemical synthesis of copper nanoparticles incorporated in poly(vinylpyrrolidone), J Nanopart Res, 10, 1183-1192.

Halimatudahliana, H.I., M. Nasir., (2003) The effect of various compatibilizers on mechanical properties of polystyrene/polypropylene blend, Polymer testing, 21, 163-170.

Hong, S.-I. and Park, W.-S., (2000) Use of color indicators as an active packaging system for evaluating kimchi fermentation, Journal of Food Engineering, 46, 67-72.

Kerry, P. , N.O'Grady, M. and Joseph, *Smart Packaging Technologies and Their Application in Conventiona lMeat Packaging Systems*. Springer Science+Business Media, LLC: 2008.

Kobayashi, Y. , Ishida, S. and Ihara, K., (2009) Synthesis of metallic copper nanoparticles coated with polypyrrole, Colloid Polym Sci, 877-880.

Lertwimolnum, W. and Vergnes, B., (2005) Influence of compatbilizers and processing conditions on the dispersion of nanoclay in a polypropylene matrix, Polymer, 46, 3462-3471.

Mirabella, F.M., *Polypropylene and thermoplastic olefins nanocomposites*. Equistar Chemicals: Cincinnati, Ohio, 2009.

Naczk, M., Towsend, M., Zadernowski, R., and Shahidi, F. (2011) Protein-binding and antioxidant potential of phenolics of mangosteen fruit, Food chemistry,

Nguyen, Q.T. and Baird, D.G., (2006) Preparation of polymer-clay nanocomposites and their properties, Polymer Technology, 25, 270-285.

Otles and Yalcin, http://www.logforum.net/vol4/issue4/no3. 2008.

Pacquit, A., Frisby, J. , Diamond, D. , Lau, K.T. , Farrell, A. , Quilty, B. and Diamond, D., (2007) Development of a smart packaging for the monitoring of fish spoilage, Food Chemistry, 466-470.

Pacquit, A., Lau, K.T. , McLaughlin, H., Frisby, J., Quilty, B. and Diamond, D. (2006) Development of a volatile amine sensor for the monitoring of fish spoilage, Talanta, 69, 515–520.

Ruparelia, J.P. , Chatterjee, A.K. , Duttagupta, S.P. and Mukherji, S., (2008) Strain specificity in antimicrobial activity of silver and copper nanoparticles, Acta Biomaterialia, 4, 707–716.

Siva, R., (2007) Status of natural dyes and dye-yielding plants in India, Current Science, 92 (7), 916-925.

Tassanawat S., M.H., Magaraphan R., and Nithithanakul M. *Polypropylene.organoclay nanocomposites for pH-sensitive packaging*; 2006.

Wu, C. , Mosher, B. and Zeng, T., (2006) One-step green route to narrowly dispersed copper nanocrystals, Journal of Nanoparticle Research, 8, 965–969.

Wu, S., (2007) Preparation of fine copper powder using ascorbic acid as reducing agent and its application in MLCC, Materials Letters, 61, 1125-1129.

Zhang, H. , Ren, X. and Cui, Z., (2007) Shape-controlled synthesis of Cu2O nanocrystals assisted by PVP and application as catalyst for synthesis of carbon nanofibers, Journal of Crystal Growth, 304, 206–210.